

ZIRCONIA BASED ORGANIC PRECURSOR INFILTRATION AS A METHOD FOR PREPARATION OF ZTA CERAMICS

PART 2 - SINTERING AND MATERIALS BEHAVIOUR

DUŠAN GALUSEK, JÁN MAJLING

*Department of Ceramics, Slovak Technical University,
Radlinského 9, 812 37 Bratislava, Slovak Republic*

Received November 30, 1995.

ZTA ceramics was prepared by infiltration of alumina matrix with organic precursors of zirconia. Alumina matrix with zirconia grains located on the grain boundaries and in triple points resulted from the procedure. The grain growth hindrance in the alumina matrix due to pinning effect of the zirconia grains was observed. This effect was pronounced at zirconia content higher than 3 vol.%. It was observed that at room temperature fine matrix microstructure favours the existence of the zirconia grains with tetragonal symmetry. However, also transformation from tetragonal to monoclinic phase was observed, so that only 20-30 vol.% of zirconia was detected in tetragonal form after 180 minutes of sintering at 1500 °C. The fracture toughness of the ZTA samples with the finest microstructure (mean grain size of alumina matrix $\approx 1.5 \mu\text{m}$) and the highest zirconia content (18 wt.%) doubled $(6.6 \text{ MPa}\cdot\text{m})^{1/2}$, compared to the fracture toughness of the alumina matrix ($\approx 3 \text{ MPa}\cdot\text{m}^{1/2}$) prepared under the same conditions. Microcracking accompanied with particle pull-out, crack deflection and crack branching were found to be the dominant mechanisms responsible for the fracture toughness enhancement.

INTRODUCTION

The improvement of the mechanical properties of ceramics for engineering applications is one of the main current tasks of material research. Several approaches were developed for the mechanical properties improvement of the ceramics. Among them, processing of ceramic fibres reinforced materials, layered materials and nanocomposites can be mentioned [1]. The preparation of transformation toughened ceramics seems also to be a promising way for reinforcing of a wide range of ceramic materials [2]. Transformation toughening is based on the transformation of metastable zirconia particles which are distributed in a ceramic matrix, to their stable monoclinic form. The transformation is triggered by the stress field in the tip of the propagating crack. Volume increase of the zirconia particles during the phase transformation generates compressive stresses in the matrix, which work against crack propagation. Enhanced fracture toughness results then from the t \rightarrow m transformation associated with the volume increase [3,4,5].

The preparation of ceramics with the highest possible content of transformable zirconia inclusions of slightly sub-critical dimensions, which are homogeneously distributed within the ceramic matrix with high elastic modulus (e.g. Al_2O_3) and ideally with higher thermal expansion coefficient than ZrO_2 is desired for the maximal fracture toughness enhancement.

The infiltration of alumina matrix with organic precursors of zirconia was tested and optimised in our previous work [6,7]. Suitability of this method for preparation of toughened ceramics is discussed in the present paper, wherein we set out to study the relations between microstructural parameters (mean grain size of alumina matrix particles and of zirconia inclusions), processing parameters (sintering) and mechanical properties of the ceramics (hardness, fracture toughness).

EXPERIMENTAL PART

The samples were prepared by liquid infiltration of porous alumina matrices with organic precursors of zirconia - zirconium n-propoxide (ZrPr) and zirconium

acetate (ZrAc). Alumina powders Martoxid ZS203^{*)} (M203, mean grain size $\approx 2 \mu\text{m}$), Baikalox CR6^{**)} (BCR6, $0.6 \mu\text{m}$) and Baikalox SM8^{**)} (BSM8, $0.2 \mu\text{m}$) were used for matrix preparation. A detailed description of the processing route (infiltration), powders and chemicals used is given elsewhere [6,7].

Infiltrated and pyrolysed samples were sintered at 1500°C , dwelling time 0 s (i.e. the heating was switched off just after 1500°C was achieved), 30, 60, 180 minutes, heating rate $10^\circ\text{C min}^{-1}$. The density of sintered samples was determined by mercury immersion method. The value of the theoretical density 3.97 g cm^{-3} for Al_2O_3 and 5.65 g cm^{-3} for ZrO_2 was taken and the rule of mixture was used to calculate the theoretical density of infiltrated samples.

The porosity and pore size distribution of the prepared specimens were measured by mercury porosimetry (Carlo Erba 1500 mercury porosimeter).

The volume ratio of tetragonal/monoclinic phase of zirconia in infiltrated and sintered alumina matrices, as well as the changes in the phase composition developed during sintering were determined by X-ray diffraction analysis. (X-ray diffractometer Dron 2.0) The volume ratio of tetragonal zirconia was calculated using integral intensities of $(111)_m$, $(111)_m$ and $(111)_t$ peaks [8].

The microstructure of sintered samples and its changes in the process of sintering as well as the influence of zirconia inclusions on the grain size of the alumina matrix were observed by means of scanning electron microscope TESLA, model BS 300 and ZEISS, model DSM 963. Samples were cut and polished to the $1 \mu\text{m}$ finish and thermally etched for 30 minutes at 1400°C . In order to evaluate the mean grain size of the alumina matrix particles as well as the zirconia inclusions, the lineal intercept method was used [9].

The hardness and fracture toughness of the samples were determined by Vickers indentation method [10] using LECO M-400-G2 indenter, maximal load used for the measurement 20 N, dwelling time at maximum load 10 s. Fracture toughness was calculated from the length of radial cracks, using equation (1) [10]:

$$K_c = \xi_v^R \left(\frac{E}{H} \right)^{1/2} \left(\frac{P}{c_0^{3/2}} \right) \quad (1)$$

where K_c - fracture toughness of the material, ξ_v^R - the experimental constant = 0.016 ± 0.004 [10], E - the Young's modulus, H - experimentally determined hardness of the material, P - maximal load, c_0 = (diagonal length of indent + length of radial cracks) / 2.

The Young's modulus was calculated from the values for crystalline alumina and zirconia obtained from [4], using the rule of mixtures.

RESULTS AND DISCUSSION

Densification

The density of the specimens determined by mercury immersion method is shown in figure 1. It shows that the relative density of porous ceramic bodies after the precursor has decomposed is growing, as it was expected, with the increasing content of zirconia in the matrix. The decrease in the porosity of the samples corresponds with the growing volume ratio of the zirconia, i.e. with the filling of the pores with precipitated zirconia.

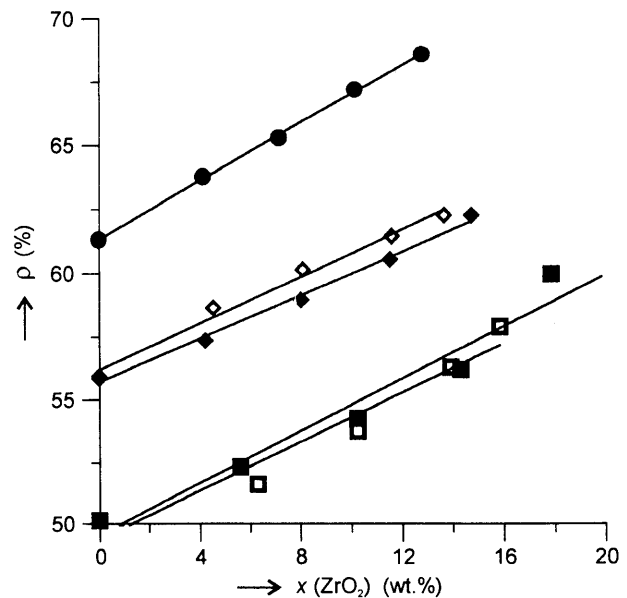


Figure 1. The density of the porous preforms after the precursor pyrolysis, as a function of zirconia content.

ρ - the relative density; $x(\text{ZrO}_2)$ - the zirconia content in the matrix; \diamond - BSM8-ZrPr; \blacklozenge - BSM8-ZrAc; \blacksquare - BCR6-ZrPr; \blacksquare - BCR6-ZrPr; \bullet - M203-ZrPr

Figure 2. shows the changes in relative density of the alumina matrices with increasing time of sintering. It is obvious from the figures, that the densification of the BSM8 matrix (mean grain size $0.2 \mu\text{m}$) is faster than for BCR6 and M203 matrices with mean grain size 0.6 and $2 \mu\text{m}$, respectively. After 0 minutes at 1500°C , 96 % of theoretical density was achieved for BSM8 matrix. The density slowly increased with prolonged sintering time. After 180 minutes of heating, 98 % of theoretical value

^{*)} Martinswerk GmbH, Germany

^{**)} Baikowski, France

was achieved. Residual porosity occurred predominantly in the form of intragranular pores (see part Microstructure, figure 5.). The densification of BCR6 matrix was slower (83 % of theoretical density after 0 minutes at 1500 °C), however, porosity less than 4 % could be achieved after 180 minutes of sintering. Even after 180 minutes of sintering at 1500 °C the M203 matrix achieved only 73 % of the theoretical density.

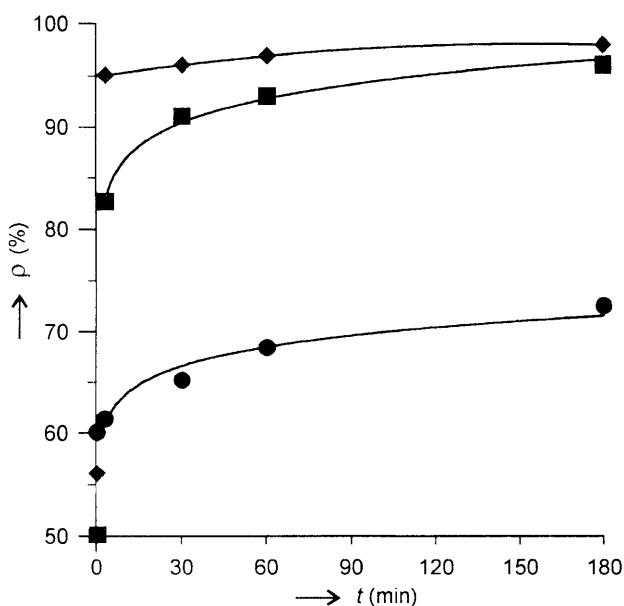
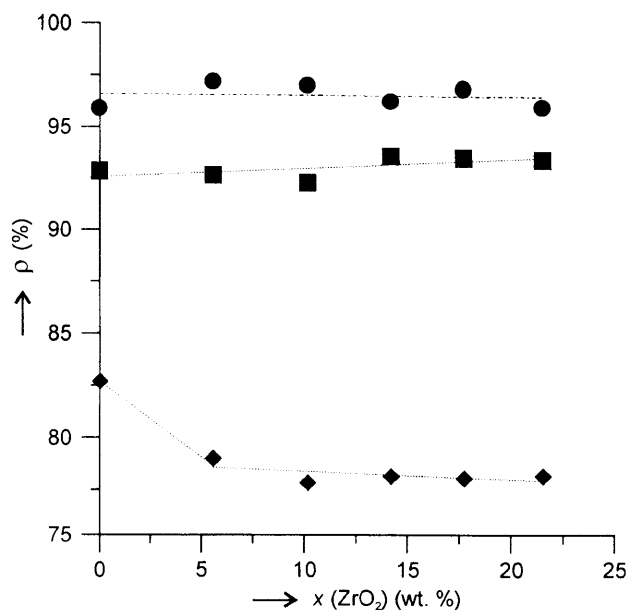


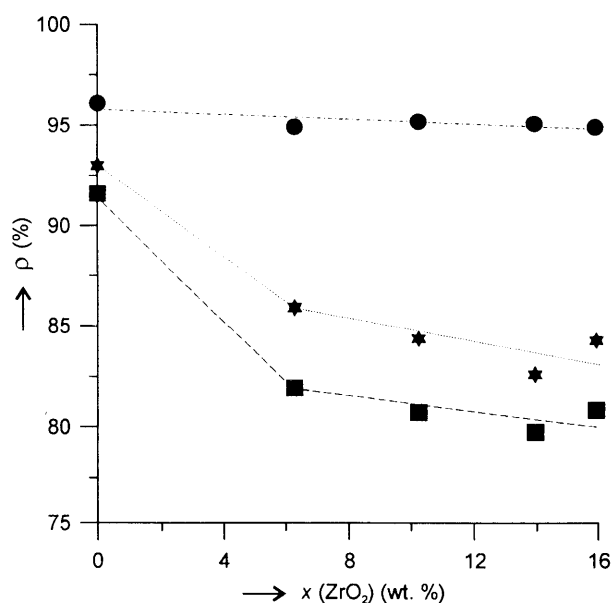
Figure 2. The dependence of the pure alumina matrix density on the time of sintering.

ρ - the relative density; t - the time of isothermal heating at 1500 °C; ● - M203; ■ - BCR6; ◆ - BSM8;

Negative influence of zirconia inclusions on densification of alumina matrix was observed, especially in the starting period of sintering (figure 3). BCR6 matrix sintered 0 minutes at 1500 °C showed the density of 83 % of theoretical value, while for the matrix containing 22 wt.% of zirconia only 77 % of theoretical density was achieved under the same conditions (figure 3a). In BSM8 matrix 92 and 81 % of theoretical density was achieved after 0 minutes of sintering at 1500 °C for the specimens containing 4 and 17 wt.% of zirconia, respectively (figure 3b). This is in agreement with the data published by Lange et al. [11]. The authors found that the pinning effect of the grains of the secondary phase(s) was responsible for the decreasing densification rate in multicomponent ceramic systems. However, we found that the influence of the zirconia inclusions is negligible in prolonged sintering. Hence, nearly no difference was observed between the relative density of pure alumina matrix and the density of zirconia doped specimens after 180 minutes of sintering.



a)



b)

Figure 3. The relative density of sintered specimens as a function of zirconia content.

a) BCR6 matrix infiltrated with ZrAc; ◆ - 1500 °C, 0 min; ■ - 1500 °C, 60 min; ● - 1500 °C, 180 min

b) BSM8 matrix infiltrated with ZrPr; ■ - 1500 °C, 0 min; ★ - 1500 °C, 120 min; ● - 1500 °C, 180 min

ρ - the relative density; $x(\text{ZrO}_2)$ - the zirconia content in the matrix

To achieve the final density >99 % of theoretical and shorten the time of sintering, porous BSM8 preforms were isostatically pressed (CIP) after the precursor pyrolysis. Pressures from 300 to 1500 MPa (step 300

MPa) were used for CIP. The samples CIPed at pressure >600 MPa reached the density $\approx 99\%$ of the theoretical after 60 minutes of sintering at 1500 °C in the whole range of tested zirconia contents (figure 4). The acceleration of densification as well as higher final density achieved can be linked to higher starting density of the samples prior to sintering. The high CIP pressures also result in extremely high pressures at the contact points of the matrix particles. It is believed that these ultra-high pressures cause an increase in the vacancies concentration within the alumina grains. In this case an additional mechanism - vacancy flow to the grain boundaries contributes to densification of the samples.

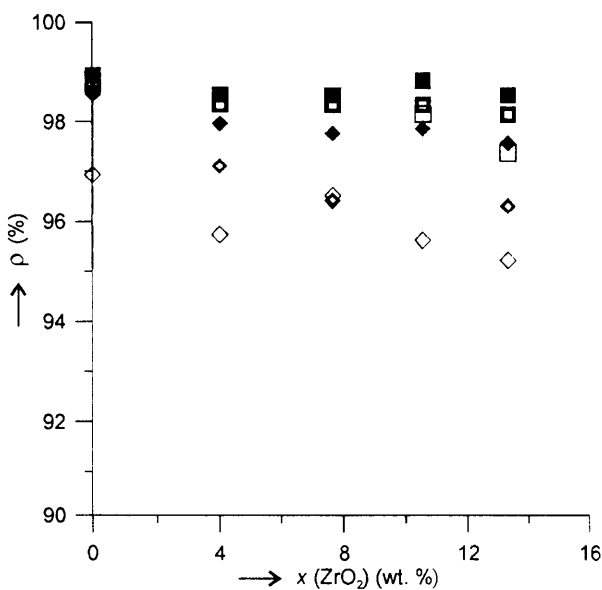


Figure 4. The final density of isostatically pressed specimens as a function of the pressure used.

ρ - the relative density, $x(\text{ZrO}_2)$ - the zirconia content in the matrix; \diamond - 0 MPa; \diamond - 300 MPa; \blacklozenge - 600 MPa; \square - 900 MPa; \square - 1200 MPa; \blacksquare - 1500 MPa

Results obtained from the density measurements can be then summarised as follows:

1. Densification of BSM8 and BCR6 matrix is finished after ≈ 180 minutes of sintering at 1500 °C, when approximately 98 and 96 % of theoretical density is achieved, respectively. Residual porosity occurs mainly in the form of intragranular pores.
2. Addition of ZrO_2 up to 16 wt.% decreases the densification rate of alumina matrix in starting period of densification. However, after 180 minutes of sintering this effect is almost negligible for the tested samples and the final density does not depend on zirconia concentration in the matrix.

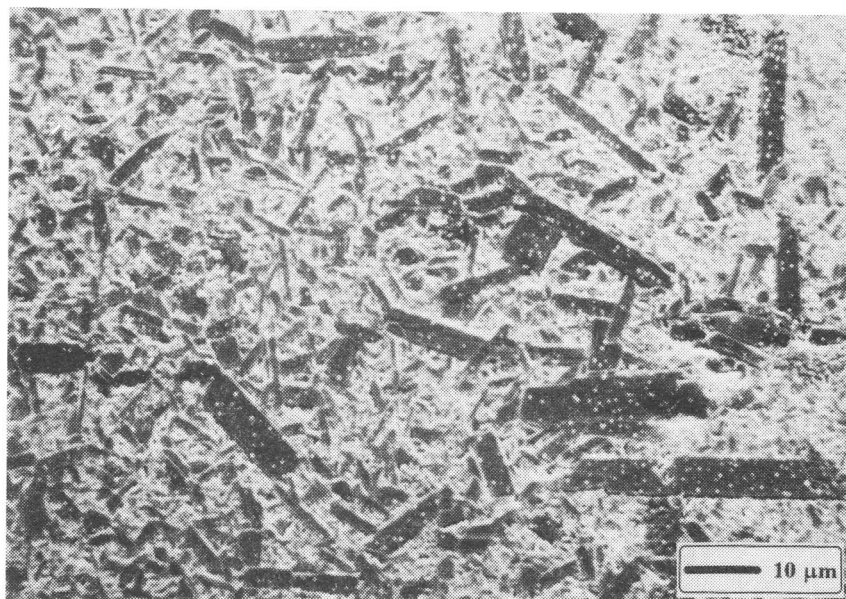
3. Application of a high pressure before sintering accelerates the densification and allows to achieve the density $\approx 99\%$ of theoretical, in the whole range of tested zirconia contents.

Microstructure

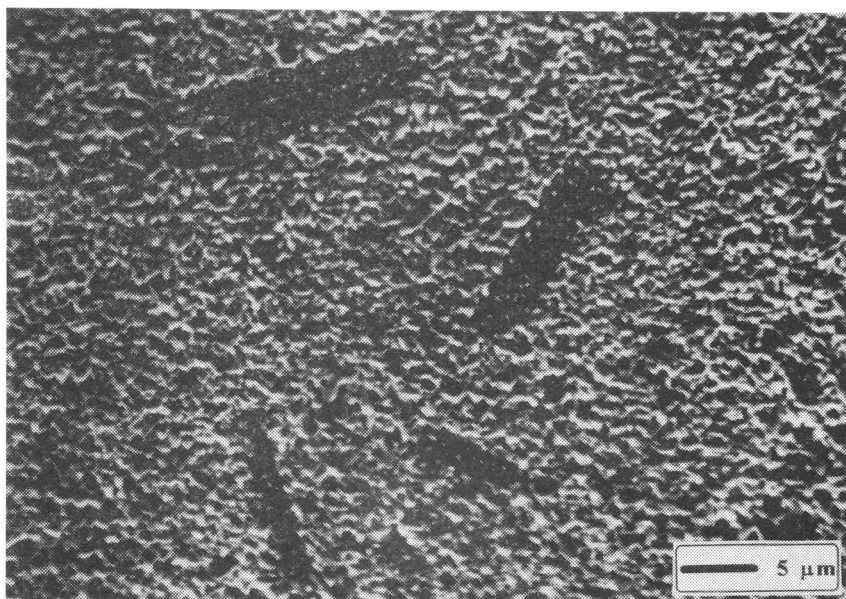
For both BCR6 and BSM8 matrices without zirconia addition, exaggerated grain growth was observed, especially for long time of sintering (180 minutes). For BSM8 sample even after 0 minutes at 1500 °C bimodal distribution of the alumina matrix particles was observed. The fraction of grains with higher mean grain size has the characteristic elongated shape (figure 5). After 180 minutes of sintering a network consisting of large grains (up to 100 μm) with elongated shape (aspect ratio ≈ 6) was observed. Intragranular pores were present within the large elongated grains (figure 5). Space between them was filled with fine fraction of isometric alumina grains. For BCR6 samples only rare occurrence of elongated grains containing intragranular pores was observed even after 180 minutes of sintering. Such a microstructure is believed to be the result of the Oswald ripening of matrix with non-homogeneously distributed large pores with low mobility [12].

Addition of 4 wt.% of zirconia was sufficient to suppress the exaggerated grain growth of alumina matrix particles, the pinning effect of zirconia grains located on the grain boundaries and in triple grain boundary junctions is believed to be the reason. Figure 6 shows the microstructure of BSM8 matrix sintered for 60 minutes at 1500 °C containing 4, 8, 11 and 14 wt.% of zirconia, respectively. The microstructure consisting of isometric alumina grains without any elongated grains was achieved. These results contradict those published by Lange and Hirlinger [13], where a minimum 5 vol.% of zirconia was supposed to be sufficient to suppress an exaggerated grain growth. For samples prepared by the infiltration, each pore originally filled with the infiltrant is occupied by nanosized zirconia particle. Hence, a lower volume ratio of zirconia is sufficient to suppress the grain growth than it was predicted by Lange and Hirlinger, [13]. Anyway, also in present work the increasing efficiency of the pinning effect with growing zirconia content was observed. The results of the mean grain size measurement are shown in figures 7a,b. A strong decrease of the mean grain size of the matrix after the first infiltration can be related to the suppression of exaggerated growth of alumina grains. Furthermore, the decrease of mean grain size with the growing zirconia content is slow but obvious.

Both the mean grain size and the number of zirconia inclusions increase with the increasing zirconia content. The inclusion size enlargement indicates that nucleation of zirconia during the precursor pyrolysis occurs not only



a)



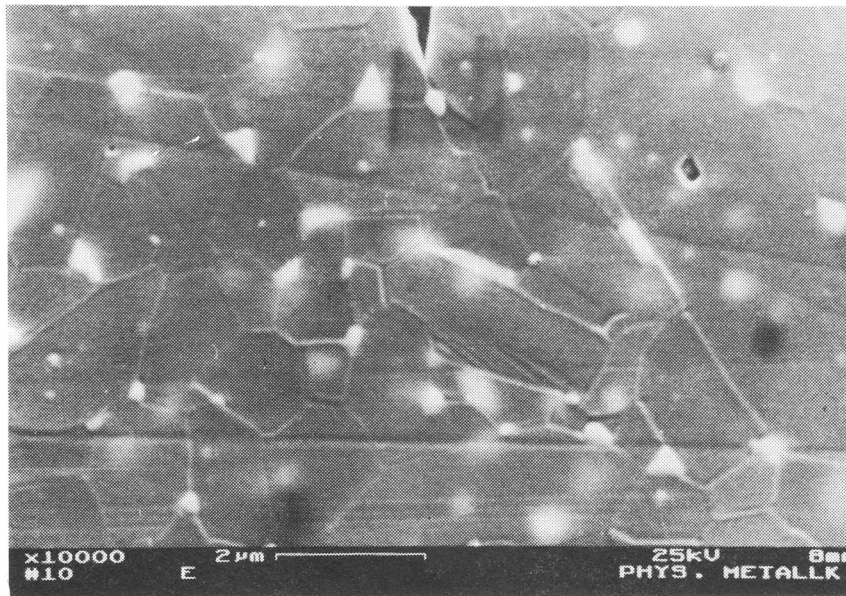
b)

Figure 5. The microstructure of the alumina matrix after 180 minutes of sintering at 1500 °C.

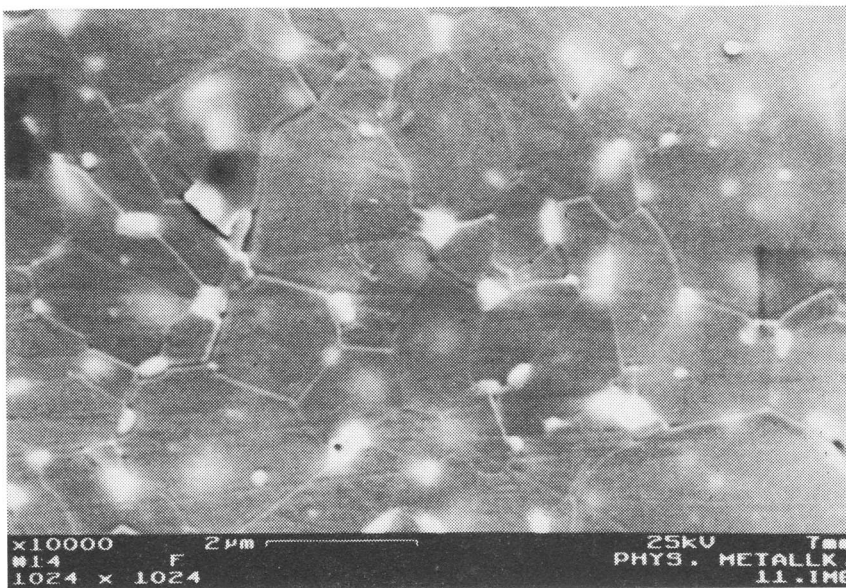
on new nucleation sites, but also on originally precipitated zirconia grains and a topotactic growth takes place.

As it was expected, the mean grain size of both alumina and zirconia grains grows with increasing time of sintering (figure 7). For alumina particles diffusion mechanisms (surface diffusion) and Oswald ripening are believed to control the grain growth. For zirconia

particles, two different mechanisms of grain growth are supposed, depending on whether the grains are located intra- or intergranularly. Intragranular inclusions with isometric (spherical or ellipsoid) shape which were found mainly in samples with low zirconia content sintered for longer times (180 minutes) grow by volume diffusion. Irregular intergranular particles located on the alumina grain boundaries result from coalescence of zirconia



a)



b)

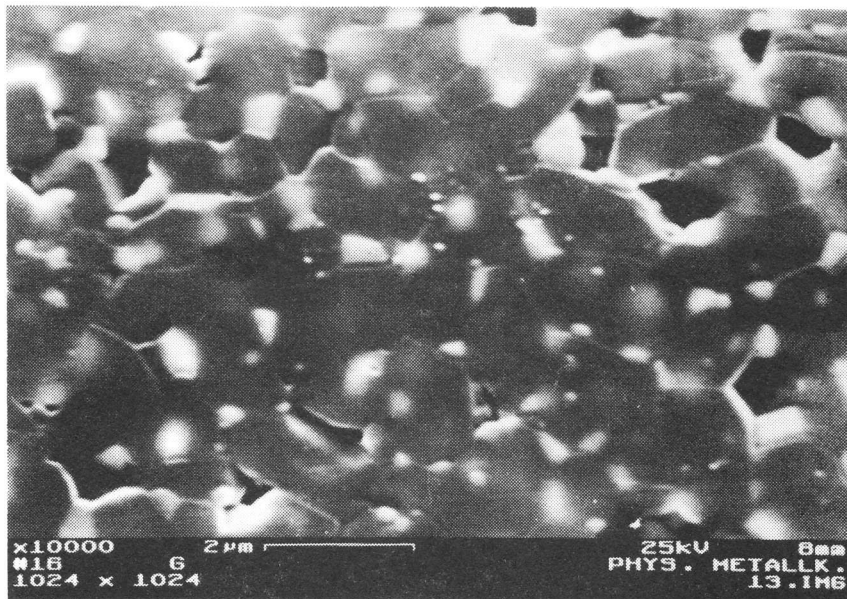
grains dragged by moving grain boundaries [14]. The grain boundary diffusion is also expected to contribute to zirconia grain growth.

The results from the microstructure investigation can be summarised as follows:

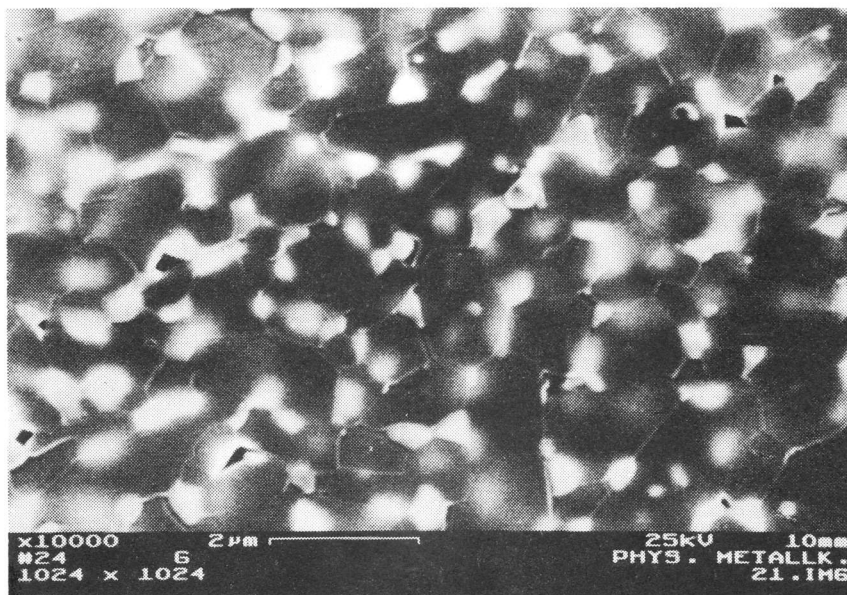
1. In the studied system, infiltration allowed to prepare $\text{Al}_2\text{O}_3\text{-ZrO}_2$ ceramics with the grains of secondary phase located mainly on grain boundaries and in

triple points. Exaggerated grain growth of the alumina grains is efficiently hindered by the zirconia addition > 4 wt. %.

2. Grain growth of zirconia and alumina particles with increasing time of sintering was observed. Zirconia grains with different morphology - isometric intragranular inclusions and irregular intergranular grains were found in the matrix.



c)



d)

Figure 6. Polished and etched cross sections through the BSM8 matrix infiltrated with ZrAc after 60 minutes of sintering at 1500 °C.
a) 4 wt.% of ZrO₂; b) 8 wt.%; c) 11 wt.%; d) 14 wt.%

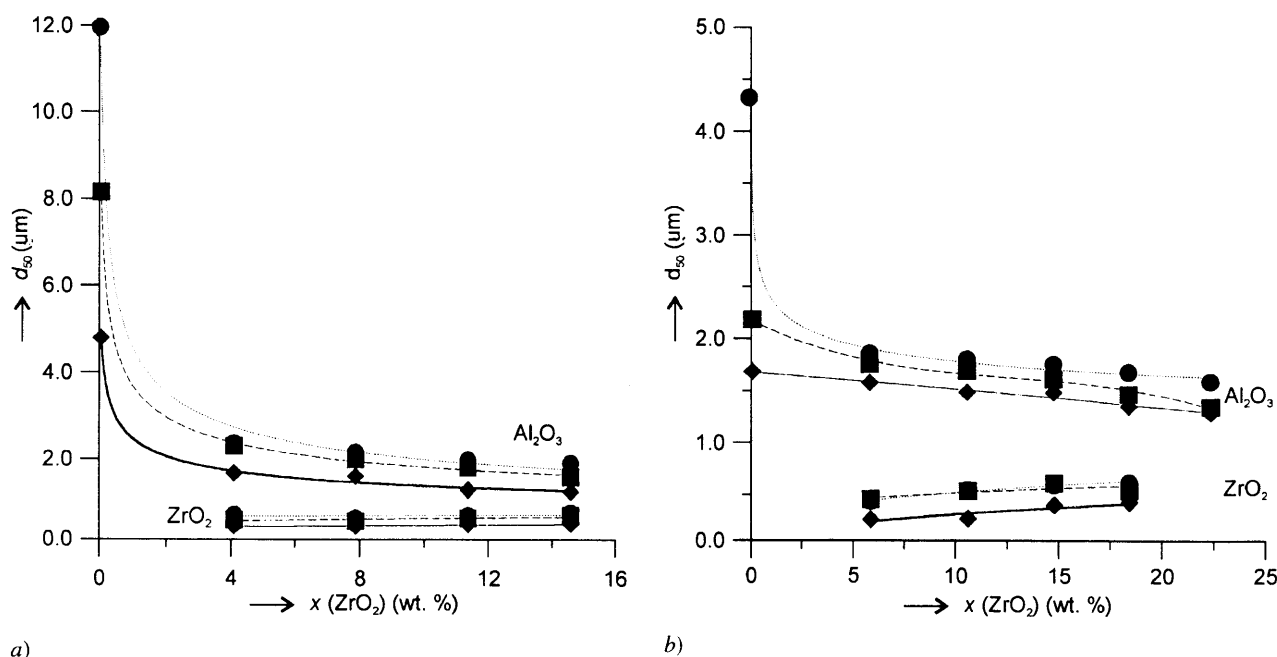


Figure 7. The mean grain size of the alumina matrix particles and precipitated zirconia inclusions measured by lineal intercept method. a) BSM8 matrix infiltrated with ZrAc; b) BCR6 matrix infiltrated with ZrAc; $x(\text{ZrO}_2)$ - the zirconia content in the matrix; d_{50} - the mean grain size of the alumina and zirconia grains.

◆ - 1500 °C, 0 min; ■ - 1500 °C, 60 min; ● - 1500 °C, 180 min

Phase composition

In the specimens tested, relatively high portion of zirconia remained in tetragonal form at room temperature, despite the fact that no stabilising agent (e.g. Y_2O_3 , CaO) was used. The content of tetragonal phase expressed in volume per cent of total zirconia content in the matrix and the matrix mean gain size are listed in table 1. The volume fraction of tetragonal zirconia depends on the mean grain size of the alumina matrix, on the number of infiltrations, as well as the kind of the precursor used. For example, in porous BSM8-ZrAc matrix after the precursor pyrolysis 86 and 80 vol.% of zirconia is present in tetragonal form after the first and fourth infiltration cycle, respectively. In the matrix with higher mean grain size (BCR6 and M203) the volume ratio of tetragonal phase decreases and in M203 (mean grain size 2 μm) only 18 and 5 vol.% of ZrO_2 is present in tetragonal form after the first and fourth infiltration, respectively. This fact can be linked to the grain size of precipitated zirconia inclusions, which depends on the pore size in the alumina matrix. Critical diameter 20 [4] and 30 nm [15] for spontaneous tetragonal \rightarrow monoclinic transformation of spherical zirconia particles at room temperature has been suggested by different authors. If

an average pore radius is known, it is possible to assess the size of precipitates with the assumption, that the precipitated particles as well as the pores are spherical and the pores are completely filled with the infiltrant. Then the radius of precipitated particle can be expressed as follows:

$$\bar{r}_z = \left((\bar{r}_p)^3 x_z \frac{\rho_i}{\rho_z} \right)^{1/3} \quad (2)$$

where \bar{r}_z - average radius of precipitated zirconia particles, \bar{r}_p - average pore radius, x_z - equivalent zirconia content in the infiltrant, ρ_i - density of the infiltrant, ρ_z - density of zirconia.

If we suppose, that no new nucleation sites are created during repeated infiltration, an average size of the precipitates after the n -th infiltration can be also expressed:

$$\bar{r}_z^{(n)} = \left(k_1 (\bar{r}_z^{(n-1)})^3 + k_2 \right)^{1/3} \quad (3)$$

where $k_1 = \left(1 - \frac{x_z \rho_i}{\rho_z} \right)$ and $k_2 = (\bar{r}_p)^3 \frac{x_z \rho_i}{\rho_z}$.

Table 1. The results of X-ray diffraction analysis of infiltrated alumina matrices after the infiltrant decomposition and crystallisation of ZrO_2 .

matrix	$d_{50}(\mu m)$	infiltrant	calc. radius of ZrO_2 (nm)		<i>t</i> - ZrO_2 content (vol.%)	
			after 1st inf.	after 4th inf.	after 1st inf.	after 4th inf.
BSM8	0.2	ZrAc	11	17	86	80
BSM8	0.2	ZrPr	12	19	72	62
BCR6	0.6	ZrAc	25	39	56	42
BCR6	0.6	ZrPr	28	43	49	42
M203	2	ZrPr	103	159	18	5

The pore size distribution measurement showed the average pore radius 33, 75 and 280 nm for BSM8, BCR6 and M203 matrices, respectively. Then, the radius of precipitated zirconia particles after the first infiltration calculated from the equation (2) is 11, 25 and 109 nm, respectively. For BSM8 and BCR6 matrix the calculated average size of zirconia grains is lower than the critical value published in literature [4, 15], what explains the higher volume fraction of the tetragonal form at room temperature for these composites, (table 1). Highly supercritical value of ZrO_2 grains in M203 matrix favours the tetragonal \rightarrow monoclinic transformation and explains low content of the tetragonal phase in this composite.

For multiplied infiltration, two effects contribute to decreasing of the tetragonal zirconia content:

1. Increasing dimensions of the precipitates (calculated size of precipitate for BSM8 matrix after the fourth infiltration is 17 nm in comparison to the precipitate size after first infiltration which is 11 nm).
2. Heating the matrix at 700 °C during the infiltrant decomposition after each infiltration cycle caused the partial recrystallization of precipitated tetragonal phase to the monoclinic one, as it was pointed out in our previous work, [7].

Higher equivalent content of ZrO_2 in ZrPr than in ZrAc precursor contributes to increasing average size of zirconia precipitates i.e. to lower volume ratio of tetragonal phase in specimens infiltrated with ZrPr.

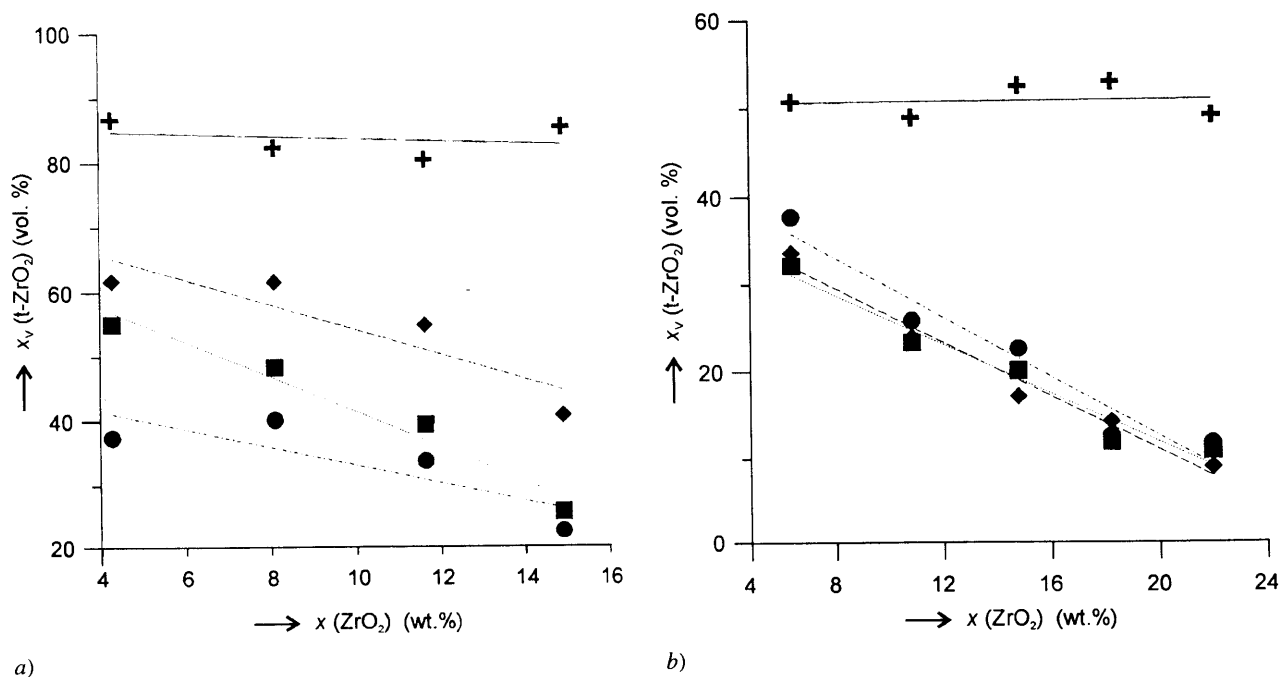


Figure 8. The content of tetragonal zirconia expressed in volume percent of total zirconia content in the infiltrated and sintered specimens.

a) BSM8 matrix infiltrated with ZrAc; b) BCR6 matrix infiltrated with ZrAc; $x(ZrO_2)$ - the total zirconia content in the matrix; $x_v(t-ZrO_2)$ - the volume fraction of tetragonal zirconia; + - 700 °C, 60 min; ◆ - 1500 °C, 0 min; ■ - 1500 °C, 60 min; ● - 1500 °C, 180 min

The results of the phase analysis of sintered samples are shown in figure 8. The content of tetragonal phase is lower in the composite sintered at 1500 °C than in porous compacts after the precursor pyrolysis at 700 °C, figure 8a. It is obvious from the figure, that the volume fraction of the tetragonal phase is influenced by the total zirconia content in the matrix after sintering as well as by the sintering time at 1500 °C. As can be seen from the mean grain size measurement (figure 7) the average size of the zirconia particles increases with increasing time of sintering. Higher zirconia content also favours the zirconia grain growth, especially by coalescence [14]. Large zirconia grains with irregular shape (figure 5) and with higher surface energy (comparing to spherical or ellipsoid grains) are easy to transform to monoclinic phase [16]. Lower volume fraction of tetragonal zirconia is then not surprising in the samples with higher total content of zirconia.

Results discussed in this part can be concluded as follows:

1. Volume fraction of tetragonal zirconia in porous compacts is influenced by the parameters which influence the mean grain size of the precipitated zirconia grains, i.e. the size of alumina matrix particles, the precursor used and the number of infiltrations.
2. In the samples sintered at 1500 °C, the volume fraction of tetragonal zirconia decreases with increasing total content of zirconia in the matrix and increasing time of sintering.

Mechanical properties

To evaluate a suitability of the infiltration method for preparation of ZTA ceramics with enhanced room temperature properties, the hardness and fracture toughness of the specimens were measured for all the composites prepared in present work. The results of these measurements are listed in tables 2 - 4.

Vickers hardness 15.1 and 16.6 GPa was determined for BSM8 matrix sintered at 1500 °C for 0 and 180 minutes, respectively. For BCR6 only 13.4 and 15.3 GPa were achieved after 60 and 180 minutes of sintering, respectively. Higher hardness values for BSM8 as well as hardness of the specimen increasing with the time of sintering can be attributed to the lower porosity of the specimens after sintering.

For all measurements performed, hardness increases in zirconia doped specimens. The highest values 18.4 and 18.0 GPa were achieved for specimens BSM8-ZrAc containing 8 and 14 wt.% of zirconia after 0 minutes of sintering at 1500 °C. This is in contrary to published data [4] where decrease of hardness with increasing zirconia content was observed due to lower zirconia hardness

comparing to pure alumina. The hardness enhancement in our case can be linked with finer microstructure of zirconia doped specimens in comparison to alumina matrix. The fact, that in specimens with highest zirconia content (14 wt.% in BSM8) lower hardness values (see table 2 - 4) were measured, also supports this idea. In these specimens the influence of lower zirconia hardness obviously prevails over the effect of finer microstructure. Furthermore, higher extent of microcracking which negatively influences the hardness [16], can be expected in the specimens with higher zirconia content, where only 20-30 vol.% of ZrO₂ is present in tetragonal form. In BCR6 samples higher porosity of sintered samples allows free expansion of zirconia inclusions during the phase transformation. Microcracking does not probably occur and monotonous enhancement of hardness with increasing zirconia content can be observed.

Table 2. The hardness and fracture toughness of BSM8-ZrPr specimens.

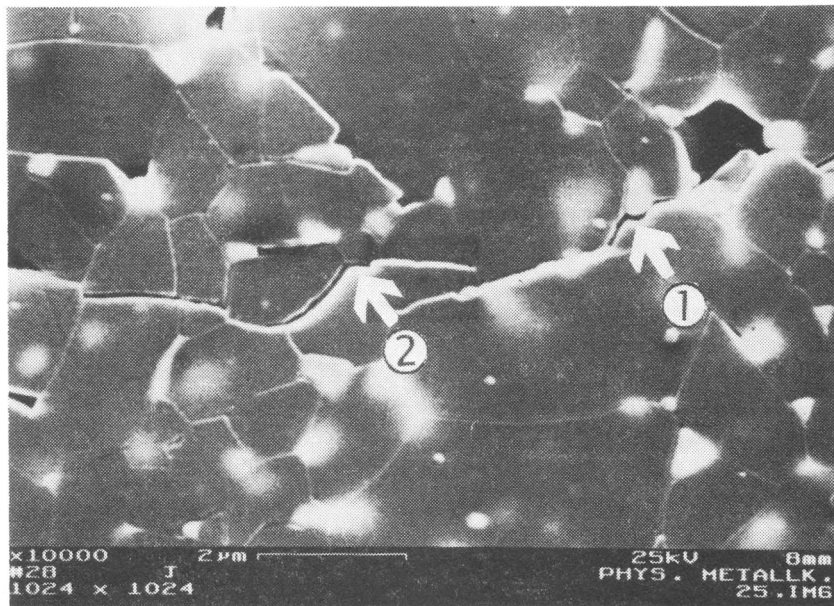
ZrO ₂ content (wt.%)	H _v (GPa)		K _{IC} (MPa m ^{1/2})	
	0 min	60 min	0 min	60 min
0	15.1 ± 0.4	15.3 ± 0.3	2.8 ± 0.2	3.2 ± 0.2
4	17.9 ± 0.1	15.4 ± 0.3	3.8 ± 0.2	3.4 ± 0.2
8	18.4 ± 0.1	16.4 ± 0.4	4.1 ± 0.4	4.1 ± 0.6
14	18.0 ± 0.3	16.0 ± 0.1	5.0 ± 0.4	5.0 ± 0.8

Table 3. The hardness and fracture toughness of BSM8-ZrAc specimens.

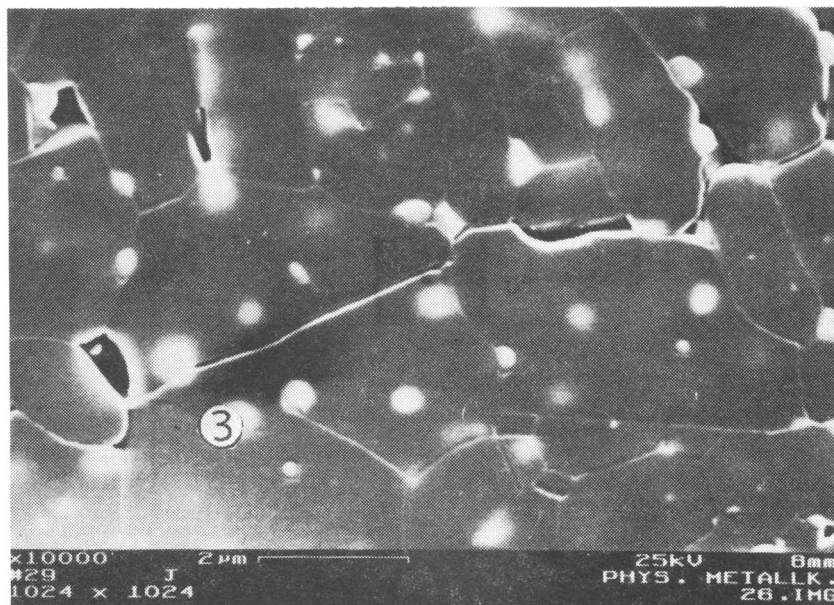
ZrO ₂ content (wt.%)	H _v (GPa)		K _{IC} (MPa m ^{1/2})	
	60 min	180 min	60 min	180 min
0	15.3 ± 0.3	16.6 ± 0.7	3.2 ± 0.2	2.6 ± 0.4
4	16.7 ± 0.3	15.9 ± 0.3	3.4 ± 0.2	3.7 ± 0.2
8	17.3 ± 0.3	16.4 ± 0.2	3.1 ± 0.2	3.5 ± 0.2
14	16.1 ± 0.2	16.8 ± 0.2	5.5 ± 0.2	4.4 ± 0.4

Table 4. The hardness and fracture toughness of BCR6-ZrAc specimens.

ZrO ₂ content (wt.%)	H _v (GPa)		K _{IC} (MPa m ^{1/2})	
	60 min	180 min	60 min	180 min
0	13.4 ± 0.2	15.3 ± 0.3	3.4 ± 0.4	2.9 ± 0.4
5	14.8 ± 0.2	17.4 ± 0.3	3.6 ± 0.2	3.6 ± 0.4
10	15.1 ± 0.4	16.7 ± 0.3	5.2 ± 0.4	4.2 ± 0.2
18	16.7 ± 0.3	15.3 ± 0.2	4.8 ± 0.4	6.6 ± 0.4



a)



b)

Figure 9. The path of propagating crack observed by SEM. Presence of the toughening mechanisms observed is marked by arrows.

a) 1 - crack deflection; 2 - crack branching; b) 3 - particle pull-out

The values of fracture toughness determined by indentation method in the present work have a relatively high error of the measurement (up to 20 rel.%). Despite of this fact, increase of the fracture toughness of tested specimens with growing zirconia content is significant. The highest value achieved for BSM8 matrix was 5.5

MPa m^{1/2} (14 wt.% of ZrO₂, sintered at 1500 °C for 60 minutes) and 6.6 MPa m^{1/2} for BCR6 (18 wt.% of zirconia, 180 minutes at 1500 °C), i.e. the obtained fracture toughness was 60 - 120 % higher comparing to pure alumina matrices prepared under the same conditions. The highest fracture toughness was achieved

in samples with the highest zirconia content, i.e. in the samples with the lowest volume ratio of tetragonal zirconia. The martensitic phase transformation then probably does not contribute substantially to fracture toughness enhancement for the composites under study. Microcracking is believed to be the major toughening mechanism contributing to increased fracture toughness. The results of the hardness measurement also support this idea because the specimens with the highest fracture toughness do not exhibit the highest hardness, table 2-4. This is in agreement with data published by Rühle & Claussen [16], where low hardness and high fracture toughness were found in microcracked samples.

Crack branching, crack deflection and particle pull-out also contribute to fracture toughness enhancement, as it was proved by SEM observations of the path of propagating crack (figure 9).

In any case, reported values of fracture toughness are relatively low comparing to the highest published data [1]. The possibilities for K_{IC} enhancement still exist, especially in the field of homogeneous macrodefect-free alumina matrix preparation. High potential is believed to be hidden in the infiltration with mixed precursors, i.e. preparation of the composites with chemically stabilised (Y_2O_3 , CaO) tetragonal zirconia of slightly subcritical dimensions. Phase transformation is expected to be a major contribution to the fracture toughness enhancement in such a material.

CONCLUSION

Development and the relations of the properties of ZTA ceramics prepared by liquid infiltration were investigated and discussed in present paper. The densification, microstructure development and mechanical properties of alumina matrix were changed by the addition of maximum 20 wt.% of ZrO_2 . The addition of 4 wt.% of zirconia suppressed an exaggerated grain growth observed in zirconia-free alumina matrix. By the presented method, the microstructure which consists of isometric alumina grains and zirconia inclusions located mainly on grain boundaries and in the triple points were prepared. The final density of the infiltrated specimens was not substantially affected by the presence of zirconia. Nearly fully dense ($\approx 99\%$ of theoretical density) ceramics with zirconia content up to 20 wt.% (20 to 80 vol.% of zirconia remained in tetragonal form at room temperature) was prepared by free sintering of porous ceramic preform at the temperature 1500 °C. For longer time of sintering (180 minutes) transformation from tetragonal to monoclinic phase occurs, so that only 20-30 vol.% of zirconia was determined in the composite in tetragonal form after the sintering. Improved hardness and fracture toughness were determined for ZTA ceramic composites. However, the maximum fracture toughness

6.6 MPa $m^{1/2}$ achieved in the present work is relatively low with respect to the highest published value 20 MPa $m^{1/2}$ [1]. Presented method has a potential to achieve a higher value of the fracture toughness by precipitation of chemically stabilised (Y_2O_3) tetragonal zirconia and by preparation of a defect free alumina body with precisely tailored pore size distribution. Higher contribution of the transformation toughening to the fracture toughness enhancement is then expected.

References

1. Evans A.G.: J.Am.Ceram.Soc. 73, 187 (1990).
2. Garvie R.C., Hannink R.H., Pascoe R.T.: Nature 258, 703 (1975).
3. McMeeking R.C., Evans A.G.: J.Am.Ceram.Soc. 65, 242 (1982).
4. Lange F.F.: J.Mater.Sci. 17, 225 (1982).
5. Heuer A.H.: J.Am.Ceram.Soc. 70, 689 (1987).
6. Galusek D., Majling J.: Ceram.Int. 21, 101 (1995).
7. Galusek D., Majling J.: Ceramics-Silikáty 39, 135 (1995).
8. Toraya H., Yoshimura M., Sômiya S.: J.Am.Ceram.Soc. 67, C119 (1984).
9. Wurst J.C., Nelson J.A.: J.Am.Ceram.Soc. 55, 109 (1972).
10. Anstis G.R., Chantikul P., Lawn B.R., Marshall D.B.: J.Am.Ceram.Soc. 64, 533 (1981).
11. Lange F.F., Yamaguchi T., Davis B.I., Morgan P.E.D.: J.Am.Ceram.Soc. 71, 446 (1988).
12. Kibbel B., Heuer A.H.: J.Am.Ceram.Soc. 69, 231 (1986).
13. Lange F.F., Hirlinger M.M.: J.Am.Ceram.Soc. 67, 164 (1984).
14. Garvie R.C.: J.Phys.Chem. 69, 1238 (1965).
15. Green D.J.: J.Am.Ceram.Soc. 65, 610 (1982).
16. Rühle M., Claussen N.: J.Am.Ceram.Soc. 69, 195 (1986).

Submitted in English by the authors.

INFILTRÁCIA KORUNDOVEJ MATRICE ORGANICKÝMI PREKURZORMI ZrO_2 AKO METÓDA NA PRÍPRAVU ZTA KERAMIKY ČÁST 2 - SPEKANIE A VLASTNOSTI MATERIÁLU

DUŠAN GALUSEK, JÁN MAJLING

*Katedra keramiky, skla a cementu CHTF STU,
Radlinského 9, 812 37 Bratislava,
Slovenská republika*

Transformačné zhúževnatie prispieva k zvýšeniu lomovej húževnatosti v materiáloch, ktoré pri laboratórnej teplote obsahujú homogénne distribuované častice tetragonálneho ZrO_2 schopné transformovať na stabilnú monoklinickú formu. Transformáciu vyvoláva tlakové pole v čele praskliny šíriacej sa cez materiál.

V prezentovanej práci bola na prípravu keramiky so zvýšenou lomovou húževnatosťou použitá kvapalinová infiltrácia korundovej matrice organickými prekurzormi ZrO_2 . Pozornosť bola zameraná najmä na schopnosť metódy zabezpečiť

homogénnu distribúciu častíc ZrO_2 ako aj optimálne fázové zloženie ZrO_2 v matrici. V práci boli zhodnotené vzťahy medzi parametrami mikroštruktúry (priemerná veľkosť častíc Al_2O_3 a ZrO_2), prípravou (dĺžka spekania) a vlastnosťami výsledného materiálu (tvrdosť, lomová húževnatosť, fázové zloženie), s cieľom dosiahnuť maximálne zvýšenie lomovej húževnatosti materiálu.

Pórovité matrice pripravené odlievaním zo suspenzie z komerčných korundových práškov, v práci označených ako BSM8, BCR6^{*)} a M203^{**)}, boli infiltrované roztokmi organických prekurzorov ZrO_2 - n-propanolátom zirkónia (ZrPr) a acetátom zirkónia (ZrAc). Po pyrolýze prekurzora boli vzorky spekané 0, 30, 60 a 180 minút pri 1500 °C, rýchlosť ohrevu 10 °C/min. Hustota spekaných vzoriek bola meraná dvojitým vážením na vzduchu a v ortuti. Fázové zloženie, t.j. podiel tetragonálnej fázy na celkovom obsahu ZrO_2 v matrici bol stanovený RTG fázovou analýzou. (Dron 2.0) Vývoj a zmeny v mikroštruktúre vzoriek boli pozorované na leštených a tepelne leptaných rezoch cez infiltrovaný objem pomocou riadkovacieho elektrónového mikroskopu (SEM) TESLA BS 300 a ZEISS DSM 963. Mechanické vlastnosti, t.j. tvrdosť a lomová húževnatosť boli merané indentačnou metódou podľa Vickersa pri maximálnom zaťažení 20N.

Z merania hustoty vzoriek vyplýva, že relatívna hustota pórovitých kompaktoz po pyrolýze prekurzora stúpa s rastúcim obsahom ZrO_2 , pričom pokles pórovitosti korešponduje s nárastom objemového zlomku ZrO_2 v matrici. (Obr.1.) Rýchlosť zhutňovania korundovej matrice počas spekania závisí od počiatočnej priemernej veľkosti častíc matrice, pričom matrice s jemnejšou počiatočnou mikroštruktúrou (BSM8) zhutňujú rýchlejšie. (Obr.2.) Prídavok ZrO_2 spôsobuje spomalenie zhutňovania materiálu v počiatočných fázach spekania. (Obr. 3), v dôsledku prekážok, ktoré vyplývajú z prítomnosti inklúzií ZrO_2 lokalizovaných na hraniciach zŕn (pinning effect). Po 180 minútach spekania pri 1500 °C bola dosiahnutá hustota maximálne 98 (BSM8), 96 (BCR6) a 73 (M203) percent teoretickej. U vzoriek, ktoré boli pred spekaním za studena izostaticky predlisované tlakmi vyššími ako 600 MPa, bolo možné v dôsledku dodatočného mechanizmu zhutňovania, ktorým je tok vakancií do fázových rozhraní, dosiahnuť hutnosti na úrovni 99 % teoretickej hustoty už po 60 minútach spekania pri 1500 °C. (Obr. 4)

Pri spekaní korundových matric bol pre obe testované vzorky (BCR6 a BSM8) pozorovaný výskyt nadmerne narastených častíc s predĺženým tvarom. Zvyšková pórovitosť bola prítomná najmä vo forme intragranulárnych pórov. U vzoriek dopovaných ZrO_2 nebol v dôsledku "pinning" efektu inklúzií ZrO_2 nadmerný rast zŕn pozorovaný, takže zrná Al_2O_3 si zachovávali izometrický tvar. (Obr. 6) Efektívnosť "pinning"

efektu sa zvyšovala s rastúcim obsahom ZrO_2 v matrici, čo sa prejavilo v zjemení mikroštruktúry a znížení priemernej veľkosti častíc Al_2O_3 . (Obr. 7)

Podiel ZrO_2 , ktorý ostával v pórovitých kompaktoch pri laboratórnej teplote prítomný v tetragonálnej forme, bol ovplyvnený parametrami, ktoré mali vplyv na veľkosť precipitujúcich častíc ZrO_2 . Takýmito parametrami boli najmä priemerná veľkosť častíc korundovej matrice (veľkosť pórových priestorov vyplnených infiltrantom), druh použitého infiltrantu (rôzny ekvivalentný obsah ZrO_2 v prekurzore) a počet opakovaných infiltrácií (zväčšovanie inklúzií ZrO_2 v dôsledku topotaktického rastu na už precipitovaných časticciach). (Tab.1) K poklesu obsahu tetragonálnej fázy počas spekania, dochádzalo najmä v dôsledku rastu zŕn ZrO_2 so stúpajúcou dĺžkou izotermickej výdrže pri 1500 °C. Rovnako vyšší celkový obsah ZrO_2 , ktorý rezultoval vo vyššej priemernej veľkosti častíc ZrO_2 (Obr. 7) spôsobil zníženie objemového zlomku tetragonálnej fázy. (Obr. 8)

Tvrdosť a lomová húževnatosť keramiky s prídavkom ZrO_2 bola u všetkých testovaných vzoriek vyššia ako tvrdosť a lomová húževnatosť korundovej matrice. (Tab. 2 - 4) Nárast tvrdosti vzoriek v dôsledku prídavku ZrO_2 možno pripísať zjemeniu mikroštruktúry vzoriek a potlačeniu nadmerného rastu zŕn. Nižšia tvrdosť ZrO_2 v porovnaní s Al_2O_3 , ako aj pravdepodobné zväčšenie rozsahu tvorby mikroprasklín sa u vzoriek s vyšším obsahom ZrO_2 prejavil opätovným znížením tvrdosti. Maximálne hodnoty lomovej húževnatosti boli dosiahnuté u vzoriek s najvyšším celkovým obsahom ZrO_2 (14 hmotn. % pre BSM8 a 18 hmotn. % pre BCR6) a boli o 60 až 120 % vyššie ako lomová húževnatosť korundovej matrice. Vysoké hodnoty lomovej húževnatosti boli teda dosiahnuté vo vzorkách s najnižším podielom tetragonálnej fázy, čo indikuje, že hlavným mechanizmom podieľajúcim sa na zvyšovaní lomovej húževnatosti bola tvorba mikrotrhlín, sprevádzaná ďalšími zhúževnaujúcimi mechanizmami (odklon trhlín, vetvenie trhlín...), pozorovanými pomocou SEM. (Obr. 9)

Na ďalšie zvýšenie lomovej húževnatosti vzoriek bude zrejme nutné zamerať pozornosť na prípravu bezdefektnej korundovej matrice s presne definovanou pórovou štruktúrou. Ďalšie možnosti pre zvýšenie hodnôt K_{IC} sú v infiltrácii korundovej matrice zmesnými prekurzormi a precipitácií chemicky stabilizovaného tetragonálneho ZrO_2 . V takomto prípade je možné očakávať výrazný príspevok transformačného zhúževnatenia k zvyšovaniu lomovej húževnatosti pripraveného materiálu.

^{*)} Baikalox SM8, Baikalox CR6, Baikowski, France

^{**)} Martoxid, Martinswerk GmbH, Germany